Published Online First: June, 2024
https://doi.org/10.21123/bsj.2024.10258
P-ISSN: 2078-8665 - E-ISSN: 2411-7986
Baghdad Science Journal

Graph Entropy of Some Special Chemical Graphs

B. I. Andrew*, *A. Anuradha*

Department of Mathematics, Faculty of Engineering and Technology, SRM Institute of Science and Technology, Kattankulathur 603203, Tamil Nadu, India.
*Corresponding Author.

Received 21/11/2023, Revised 28/04/2024, Accepted 30/04/2024, Published Online First 20/06/2024

Abstract

Chemical graph theory plays an important role in modelling molecules, especially examining physico-chemical properties of the chemical compounds. Alkanes are one of the chemical compounds which are made up of hydrogen and carbon atoms, generally known as hydrocarbons. These alkanes having empirical formula $C_nH_{2(n+1)}$. Structural/constitutional isomers are the collection of chemical compounds having same empirical formula but different structural arrangements, this lead to the diversity in the physico-chemical properties. Graph descriptors are the essential tools in the graph theory to study about these physico-chemical properties. Some of these graph descriptors are graph spectrum, graph energy and graph entropy which contribute significantly to understand molecular properties. Spectral parameters, like spectral radius, second largest eigenvalue, spectral gap and graph energy aid in estimating energy levels and stability of the molecule, while graph entropy, such as eigenvalue-based modulus entropy derived from the adjacency matrix, measure heterogeneity. This paper explores a specific type of alkanes and their isomers, examining their spectral parameters and graph entropy. Through comparative graph plots, the nature of these parameters are observed, which sheds light on the molecular behaviours. This study shows the importance of graph theory in quantum chemistry, particularly the spectral characteristics and structural intricacies of alkanes and their isomers, contributing to a comprehensive understanding of molecular properties and behaviour at the quantum level.

Keywords: Alkane Isomers, Caterpillar Graph, Eigenvalue-based Modulus Entropy, Graph Energy, Graph Spectrum.

Introduction

Chemical graph theory is a branch in graph theory which deals with the application of the concept of graph theory in the field of chemistry, which depict the structural arrangement of molecules. Cheminformatics employs various approaches to analyse and represent molecular structures. One widely used method is the utilization of graph-theoretical descriptors or indices to depict the physical characteristics of molecules. Among these descriptors, the spectrum of the graph plays a crucial role in estimating the highest energy levels of molecules in quantum chemistry. Additionally, graph entropies[2] are fundamental thermophysical quantities used to measure the heterogeneity and relative stabilities of molecules and are defined for various graph invariants. Eigenvalue-based modulus entropy, a kind of graph entropy that depends on the adjacency matrix of the graph, has been extensively studied.

Physico-chemical characteristics of a chemical compound are related to the compound's geometric structure. This is particularly true for chemical substances known as alkanes. Alkanes are a type of hydrocarbons (i.e. contain only carbon and

Published Online First: June, 2024
https://doi.org/10.21123/bsj.2024.10258
P-ISSN: 2078-8665 - E-ISSN: 2411-7986
Baghdad Science Journal

hydrogen atoms) with the relation between their elements as n carbon atoms and $2n+2$ hydrogen atoms. Methane, ethane, propane and butane are a few of these alkanes that are widely known. Chemical trees are molecular graphs in which the bonds between the carbon atoms are considered as edges and the carbon atoms alone are taken as vertices. For example, isomers of alkanes like 2,2-dimetylpropane (2,2m-3) and 2,2,3,3-tetramethylbutane (2,2,3,3m-4) exhibit molecular graph in such a way that each internal vertex of the central path (called the spine) is adjacent with two pendant vertices, forming a special kind of caterpillar graph CP_n. In this study, the spectral parameters and graph entropy of the caterpillar graph CP_n were determined and represented in graphical form for easy analysis.

Preliminaries

A collection of two sets: a nonempty set of vertices V, a set of edges E and a relation $\psi_G: E \to V \times V$ called incidence relation arranged as an ordered triplet (V, E, ψ) is called as a graph and is notated as $G = (V, E, \psi)$. The adjacency matrix $A(G)$, also referred to as the connection matrix, is a square matrix that indicates whether or not the two vertices v_i, v_j are adjacent neighbours. All the ij-elements of $A(G)$ are marked as 1 in the matrix if their corresponding vertices are neighbours. Otherwise, mark it as 0. $P(A;\lambda) = det(A - \lambda I_n)$ yields the characteristic polynomial of $A(G)$, where I_n is the identity matrix. The eigenvalues of the adjacency matrix $A(G)$ are determined by solving the characteristic equation $P(A;\lambda) = 0$. The spectrum of the graph G is the configuration of the eigenvalues and their algebraic multiplicities. The highest among all the eigenvalues is known as spectral radius. The sum of absolute eigenvalues is termed as graph energy[3]. The difference between spectral radius and the second largest eigenvalue is known as the spectral gap. If $\lambda_1, \lambda_2, \dots, \lambda_n$ denote the eigenvalues of $A(G)$ and $\mathcal{E}(G)$ denote the energy of G, then the eigenvalue-based modulus entropy[4] of G is defined as $I(A) = -\sum_{j=1}^{n} \frac{|\lambda_j|}{E(G)} log \frac{|\lambda_j|}{E(G)}$. Closed neighbourhood $N_G[e]$ of an edge e refers to a set of all edges which are adjacent to a particular edge e including the edge itself. An independent set of edges is a set of edges such that no two edges share a common vertex. Matching is an independent set of edges. A k-matching comprises k edges in its matching and the matching with the highest cardinality is known as a maximum matching M of G.

Literature survey

In the book Spectra of Graphs, A. E. Brouwer and W. H. Haemers[5] explore a wide range of subjects in spectral graph theory and show how crucial a role linear algebra plays in graph theory. F. Celik and I.N. Cangul[6] have shown that one may derive the spectra of C_{2n} and P_{2n+1} without performing intricate computations only in terms of the spectra of C_n and P_n. They did this by obtaining the polynomials and recurrence relations for the spectral polynomials of cycles and routes. N. A. Alwan and N. M. G. Al-Saidi[7] have provided a general formula for the characteristic equation of various well-known graphs, such as cycle, path, star and complete graphs. Ivan Gutman et al[8] have proposed a novel approach for approximating the total pi-electron energy of a conjugated hydrocarbon using spectral moments. Anwar S[9] et al has investigated the extreme value of the first reformulated Zagreb index with a given order and degree of a graph. Further, they have presented the regression models to predict acentric factor and entropy of octane isomers. Mitesh JP et al[10] has derived the relation between the second Zagreb matrix and the adjacency matrix of graph G and derive the new upper bound for the second Zagreb energy in the context of trace. Similar interesting studies regarding various indices are addressed in[11-13]. H. Al-Janabi and G. Bacsó[14] have found Sanskruti Index for the caterpillar tree, cycle-caterpillar, starlike tree, sunlike graph and molecular graphs of hydrocarbons. Zhen L[15] has focused on how to use fewer topological indices to predict the physicochemical properties of compounds through the QSPR analysis of connectivity indices of benzene hydrocarbons. Z Ahmadet. al[16] computed some eccentric connectivity indices of the V-Phenylenic nanotube VPHX[p;q]. N. J. M. M. Raja and A. Anuradha[17] have computed the Sombor index, reduced Sombor index and average Sombor index of armchair and zigzag carbon nanotubes. N. J. M. M. Raja and A. Anuradha[18] have established the Sombor indices of tensor product and 2-tensor product of certain families of graphs. Devaragudi V, Chaluvaraju[19] has obtained some bounds and characterizations of Block Somber Index and its Block Sombor energy. M. K. Jamil et al[20] reveals a strong correlation (r > 0.99) between a novel topological index in multiple linear regression and

Published Online First: June, 2024
https://doi.org/10.21123/bsj.2024.10258
P-ISSN: 2078-8665 - E-ISSN: 2411-7986
Baghdad Science Journal

the prediction of π-electron energy and boiling points in benzenoid hydrocarbons. Additionally, the index shows promising results in analyzing face indices of planar molecular structures like 2-dimensional graphene and circumcoronene series, indicating its potential as a valuable parameter in QSPR/QSAR with excellent correlation ability and structural selectivity. X. Zhang et.al [21], has investigated the degree-based entropies: geometric arithmetic entropy, atom bond connectivity entropy, general Randic′ entropy, and general sum connectivity entropy for metal–organic network. M.S. Sardar et al[22] has calculated certain well-known topological indices of the middle graph of alkane based on vertex degree and presented a numerical and graphical comparison of computed topological indices. M. S. Sardar et al[23] has computed many topological indices for the double and strong double graph of alkane. M. P. Nayaki et al[24] has studied the diagrammatic representation between Topological indices and 67 Alkanes. K.V. Lakshmi, N. Parvathi[25] has computed the sombor index, harmonic index, inverse sum index and symmetric division degree index of a thorn graph family. M. Javaid et al[26] has established the numerical relationship between the Gutman connection (GC) index of a graph and its thorn graph. K. Chithra, J. Mayamma[27] has calculated the total global dominator chromatic number of trees and unicyclic graphs are explored. A. M. Ali[28] has found the polynomials detour and detour indices for n-graphs, which are connected to themselves and separated from each other with respect to the vertices for $n \geq 3$, having important applications in Chemistry.

Molecular Graph of Alkane Isomer

In organic chemistry, alkanes are acyclic saturated hydrocarbons[29]. It is made up of carbon and hydrogen atoms that are arranged in a tree structure with only single carbon-carbon bonds. It has the chemical formula C_nH_{2n+2} with $n \geq 1$. The first four alkane are methane, ethane, propane, and butane. After that, the alkanes are named based on Greek numbers. For example, C_5H_{12} is pentane, C_6H_{14} is hexane, C_7H_{16} is heptane and C_8H_{18} is octane etc. According to the branching of the carbon atoms, each alkane may have many isomers. As these isomers vary in their basic structure, they exhibit different properties though belonging to the same alkane group. Depending on the context, a particular isomer of an alkane will be chosen for use. The compound pentane C_5H_{12} has three isomers: n-pentane, isopentane and neopentane. The first two are liquids while the third is a gas. Neopentane is a double-branched chain alkane with five carbon atoms, commonly known as 2,2-dimethylpropane (2,2m-3) (Fig 1)[23] . It is a flammable gas at room temperature which condense into a highly volatile liquid when it is compressed to a higher pressure. The molecular graph of neopentane (2,2m-3) can be drawn in the form of caterpillar graph CP_3 in such a way that the central path (spine) contains three vertices, and its single internal vertex has 2 pendant vertices adjacent with it.

(a) 2,2-dimetylpropane (b) Caterpillar graph (CP_3)

Figure 1. Molecular graph of (2,2m-3)

When a similar structure is seeked in the alkane octane, 2,2,3,3-tetramethylbutane (2,2,3,3m-4) is there with similar structure and chemical formula C_8H_{18}. Among the several octane isomers, it has the most branches with chemical formula C_8H_{18}. It is also the only one with a butane (C_4) backbone. It is the smallest saturated acyclic hydrocarbon that solidifies at $25°C$ due to its highly symmetrical structure, which also gives it a very high melting point and a small liquid range. The molecular graph of (2,2,3,3m-4) is the caterpillar graph CP_4 (see Fig 2) [23] .

(c)2,2,3,3-tetramethylbutane (d) Caterpillar graph (CP_4)

Figure 2. Molecular graph of (2,2,3,3m-4)

On generalizing the structure of the caterpillar graph CP_n, the spine of CP_n contains n vertices, and $2(n-2)$ pendant vertices adjacent to the internal vertices of the spine. As a result, the Caterpillar graph CP_n contains $(3n-4)$ vertices and $(3n-5)$ edges. The caterpillar graph CP_n for $3 \leq n \leq 10$ and their corresponding alkane isomer is listed in Table 1.

Published Online First: June, 2024
https://doi.org/10.21123/bsj.2024.10258
P-ISSN: 2078-8665 - E-ISSN: 2411-7986
Baghdad Science Journal

Table 1. Caterpillar graph CP_n, $3 \leq n \leq 10$, and its corresponding Alkanes

CP_n	Alkanes
CP_3	2,2-dimethylpropane (2,2m-3)
CP_4	2,2,3,3-tetramethylbutane (2,2,3,3m-4)
CP_5	2,2,3,3,4,4-hexamethylpentane (2,2,3,3,4,4m-5)
CP_6	2,2,3,3,4,4,5,5-octamethylhexane (2,2,3,3,4,4,5,5m6)
CP_7	2,2,3,3,4,4,5,5,6,6-decamethylheptane (2,2,3,3,4,4,5,5,6,6m7)
CP_8	2,2,3,3,4,4,5,5,6,6,7,7-dodecmethyloctane (2,2,3,3,4,4,5,5,6,6,7,7m8)
CP_9	2,2,3,3,4,4,5,5,6,6,7,7,8,8-tetradecmethylnonane (2,2,3,3,4,4,5,5,6,6,7,7,8,8m9)
CP_{10}	2,2,3,3,4,4,5,5,6,6,7,7,8,8,9,9-hexadecmethyldecane (2,2,3,3,4,4,5,5,6,6,7,7,8,8,9,9m10)

Materials and Methods

Algebraic Properties of CP_n

Consider the Caterpillar graph CP_n $(n \geq 3)$ (Fig 3) [11]. Let $V(CP_n) = \{u_i, 1 \leq i \leq n\} \cup \{v_i, w_i, 1 \leq i \leq n-2\}$ be the vertex set. Here u_i are the vertices of the spine, v_i and w_i are pendant vertices. The vertices v_i and w_i are adjacent with each u_{i+1}, $1 \leq i \leq n-2$. Let $E(CP_n) = \{u_i u_{i+1} = e_{u_i}, 1 \leq i \leq n-1\} \cup \{u_{i+1} v_i = e_{v_i}, u_{i+1} w_i = e_{w_i}, 1 \leq i \leq n-2\}$ be the edge set. With respect to the labellings of edges, partition $E(CP_n)$ into $Q_1 = \{e_{u_1}, e_{u_2}, e_{u_3}, \dots, e_{u_{n-1}}\}$, $Q_2 = \{e_{v_1}, e_{v_2}, e_{v_3}, \dots, e_{v_{n-2}}\}$ and $Q_3 = \{e_{w_1}, e_{w_2}, e_{w_3}, \dots, e_{w_{n-2}}\}$. Clearly both Q_2 and Q_3 are independant sets.

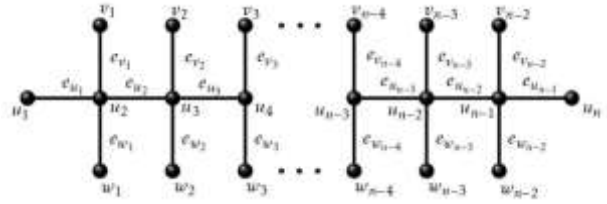

Figure 3. Caterpillar graph (CP_n)

Lemma 1[30]. *Let G be a labelled simple graph on n vertices. If L_i denotes the collection of i-vertex graphs whose components are edges or cycles, and a_i denotes the coefficient of λ^{n-i} in the characteristic polynomial of G, then*

$$a_i = \sum_{L \in L_i} (-1)^{c(L)} 2^{y(L)},$$

where $c(L)$ is the number of components of L and $y(L)$ is the number of components which are cycles.

Lemma 2[7] *The coefficients of the characteristic polynomial of path graph (P_n) based on $A(P_n)$ is given by*

$$P_{P_n}(A, \lambda) = \binom{n}{n}\lambda^n - \binom{n-1}{(n-1)-1}\lambda^{n-2} + \binom{n-2}{(n-2)-2}\lambda^{n-4} - \binom{n-3}{(n-3)-3}\lambda^{n-6} + \cdots \pm 1.$$

Theorem 1 *The Adjacency matrix $A = A(CP_n)$ is given by*

$$A(CP_n) = \begin{bmatrix} 0_{2\times 2} & E_{11,2(n-2)} & 0_{2\times(n-2)} & 0_{2\times(n-2)} \\ E_{11,(n-2)2} & P_{n-2} & I_{n-2} & I_{n-2} \\ 0_{(n-2)\times 2} & I_{n-2} & 0_{(n-2)\times(n-2)} & 0_{(n-2)\times(n-2)} \\ 0_{(n-2)\times 2} & I_{n-2} & 0_{(n-2)\times(n-2)} & 0_{(n-2)\times(n-2)} \end{bmatrix},$$

where $0_{2\times 2}$ and $0_{(n-2)\times(n-2)}$ are null matrices; $E_{11,2(n-2)}$ and $E_{11,(n-2)2}$ are the matrices with order $2 \times (n-2)$ and $(n-2) \times 2$ respectively in which the entries a_{11} , $a_{2(n-2)}$ of $E_{11,2(n-2)}$ are 1, the entries a_{11} , $a_{(n-2)2}$ of $E_{11,(n-2)2}$ are 1 and otherwise 0; P_{n-2} is the adjacency matrix of the path graph having $(n-2)$ vertices; I_{n-2} is the identity matrix.

Proof. As the pendant vertices in the spine are not adjacent, the main diagonal's first block null matrix of order 2×2 is formed. A path adjacency matrix P_{n-2} is formed from the spine's subsequent vertices from u_3 and u_n. Due to the fact that the vertices v_{i-2} and w_{i-2} are pendant and adjacent with the vertices of the spine, two consecutive null block matrices of order $n-2$ are formed in the main diagonal. Additionally, the adjacent pairs (u_1, u_3) and (u_2, u_n) create the block matrix $E_{11,(n-2)2}$ to the left of P_{n-2} with order $(n-2) \times 2$, where the elements

Published Online First: June, 2024
https://doi.org/10.21123/bsj.2024.10258
P-ISSN: 2078-8665 - E-ISSN: 2411-7986
Baghdad Science Journal

a_{11} , $a_{(n-2)2}$ of the matrix are 1. Due to their pendant nature and proximity to the spine's vertices, v_{i-2} and w_{i-2} produce two successive identical block matrices just below P_{n-2}. The blocks above the diagonal follows because of the symmetry of the adjacency matrix.

Theorem 2 *Let P_n where $(n \geq 1)$ be the path graph then the number of k- matching is given by $\binom{n-k}{n-2k}$ for any positive integer k.*

Proof. By using Lemma 2,

$$P_{P_n}(A,\lambda) = \binom{n}{n}\lambda^n - \binom{n-1}{(n-1)-1}\lambda^{n-2} + \binom{n-2}{(n-2)-2}\lambda^{n-4} - \binom{n-3}{(n-3)-3}\lambda^{n-6} + \cdots \pm 1.$$

$$= \binom{n}{n}\lambda^n - \binom{n-1}{n-2}\lambda^{n-2} + \binom{n-2}{n-4}\lambda^{n-4} - \binom{n-3}{n-6}\lambda^{n-6} + \cdots \pm 1.$$

Since, the path graph is acyclic then by Lemma 2 the coefficients of its characteristic polynomial will be k - matching of path graph and thus the theorem follows.

Theorem 3 *A maximum matching M of a path graph P_n will always have the following number of edges in it $|M| = \left\lfloor \frac{n}{2} \right\rfloor$.*

Proof. An alternate selection of edges, starting from the first edge of the path P_n, will form a maximum matching with $\left\lfloor \frac{n}{2} \right\rfloor$ edges.

Theorem 4 *If CP_n is the caterpillar graph with $n \geq 3$, then the number of 2-matchings is $\frac{9n^2-45n+54}{2}$.*

Proof. For each internal edge of the spine P_n, $N_G[e_{u_i}] = \{e_{u_i}, e_{u_{i-1}}, e_{u_{i+1}}, e_{v_{i-1}}, e_{v_i}, e_{w_{i-1}}, e_{w_i}\}$ and hence $|N_G[e_{u_i}]|$ =7 for $2 \leq i \leq n-2$. Omitting these 7 closed neighbourhood edges from the $E(CP_n)$, $(3n-12)$ edges will be obtained, each of which will form a 2-matching with e_{u_i}. Since there are $(n-3)$ internal edges e_{u_i}, $(n-3)(3n-12)$ 2-matchings will be formed. Each of the remaining edges in the collection $X = \{e_{u_1}, e_{u_{n-1}}, e_{v_i}, e_{w_i}, 1 \leq i \leq n-2\}$ will have four edges in its closed neighbourhood set. By omitting these corresponding closed neighbourhood edges from $E(CP_n)$, $(3n-9)$ edges will be obtained, which forms a 2-matching. There are $(2n-2)$ such edges in collection X. Thus $(2n-2)(3n-9)$ 2-matchings will be fromed from collection X. By summing up, will get $9n^2-45n+54$ 2-matchings. The result is then halved to avoid repetition. Thus $\frac{9n^2-45n+54}{2}$ 2-matchings is obtained.

Theorem 5 *The Caterpillar graph CP_n has a maximum matching M with exactly $(n-2)$ edges.*

Proof. Consider the partition $Q_2 \subset E(CP_n)$ with $|Q_2| = (n-2)$. It is observed that $N_G[Q_2] = E(CP_n)$. Additionally, when introducing any spine edge to Q_2, it necessitates the removal of at least two Q_2 edges to form a matching. Consequently, defining a matching larger than Q_2 is unfeasible. Hence, CP_n possesses a maximum matching of cardinality $(n-2)$. As $|Q_2| = |Q_3|$, Q_3 also qualifies as a maximum matching of CP_n, thereby establishing the theorem.

Algorithm to Enumerate k-matchings of CP_n

Proceeding to calculate the number of k-matchings in CP_n, where $3 \leq k \leq n-3$ is the focus. This is done by the following manner. The partitions are paired in the following ways: (Q_1, Q_2), (Q_1, Q_3), (Q_2, Q_3) and (Q_1, Q_2, Q_3). Then k-matchings of each pair are computed and added to form the whole k-matching collection.

Step 1: The first step is to compute all k-matchings that lie in one partition itself. By using Theorem 2 the k-matching from the partition Q_1 can be found. As previously mentioned, Q_2 and Q_3 are independant edge sets, thus the k-matching can be found by collecting all k combinations.

Step 2: The selection of matching edges depends on the number of coupled partitions. For instance, to pair two partitions, i edges are chosen from one partition and $k-i$ edges from another. Similarly, for pairing three partitions, i edges from the first partition, j edges from the second, and $k-i-j$ edges from the third are selected. The identification of each partition's suitable matching is determined by the properties of the edges within that partition. When searching for matches in a partition, edges adjacent to those in the preceding partitions are excluded.

Step 3: Let M be a maximum matching of CP_n with $|M|$ edges and M_1 be a k-matching with $|M_1| = k$

Published Online First: June, 2024
https://doi.org/10.21123/bsj.2024.10258
P-ISSN: 2078-8665 - E-ISSN: 2411-7986
Baghdad Science Journal

edges. The internal edges $e_{u_i}, 2 \le i \le n-2$ in partition Q_1 are all adjacent with two edges in partitions Q_2 and Q_3, but the remaining two edges e_{u_1}, $e_{u_{n-1}}$ in Q_1 are adjacent with one edge in Q_2 and Q_3 (refer Fig 3)[9]. Thus obtain four cases while coupling the other partition with Q_1.

(a) If $e_{u_1}, e_{u_{n-1}} \notin M_1$ (b) If $e_{u_1} \in M_1, e_{u_{n-1}} \notin M_1$ (c) If $e_{u_1} \notin M_1, e_{u_{n-1}} \in M_1$ (d) If $e_{u_1}, e_{u_{n-1}} \in M_1$.

Partition of i edges

1) Partition (Q_1, Q_2)

***Case* (i) *If* $e_{u_1}, e_{u_{n-1}} \notin M_1$.**

(a) *If* $3 \le k \le \left\lfloor \frac{|M|+1}{2} \right\rfloor$, then $\sum_{i=1}^{k-1} \binom{n-2-i}{n-2-2i}\binom{n-2-2i}{k-i}$

(b) *If* $k \le |M| - r$, *where* $r = 1,2,3,\dots,\left\lfloor \frac{|M|-2}{2} \right\rfloor$, *then* $\sum_{i=1}^{r} \binom{n-2-i}{n-2-2i}\binom{n-2-2i}{k-i}$.

(c) *If* $k = |M|$ *then* $(Q_1, Q_2) = 0$.

***Case* (ii) *If* $e_{u_1} \in M_1, e_{u_{n-1}} \notin M_1$ *or* $e_{u_1} \notin M_1$, $e_{u_{n-1}} \in M_1$.**

(a) *If* $3 \le k \le \left\lfloor \frac{|M|+2}{2} \right\rfloor$, *then* $2\sum_{i=1}^{k-1} \binom{n-3-(i-1)}{n-3-2(i-1)}\binom{n-3-2(i-1)}{k-i}$.

(b) *If* $k = |M| - r$, *where* $r = 0,1,2,3,\dots,\left\lfloor \frac{|M|-3}{2} \right\rfloor$, *then*

$$(Q_1, Q_2) = 2\sum_{i=1}^{r+1} \binom{n-3-(i-1)}{n-3-2(i-1)}\binom{n-3-2(i-1)}{k-i}.$$

***Case* (iii) *If* $e_{u_1}, e_{u_{n-1}} \in M_1$.**

(a) *If* $3 \le k \le \left\lfloor \frac{|M|+2}{2} \right\rfloor$, *then* $\sum_{i=1}^{k-1} \binom{n-4-(i-2)}{n-4-2(i-2)}\binom{n-4-2(i-2)}{k-i}$.

(b) *If* $k \le |M| - r$, *where* $r = 0,1,2,3,\dots,\left\lfloor \frac{|M|-3}{2} \right\rfloor$, *then*

$$(Q_1, Q_2) = \sum_{i=1}^{r+2} \binom{n-4-(i-2)}{n-4-2(i-2)}\binom{n-4-2(i-2)}{k-i}.$$

2) Partition (Q_1, Q_2, Q_3)

***Case* (i) *If* $e_{u_1}, e_{u_{n-1}} \notin M_1$.**

(a) *If* $3 \le k \le \left\lfloor \frac{|M|+2}{2} \right\rfloor$, *then* $\sum_{i=1}^{k-2} \binom{n-2-i}{n-2-2i}\left(\sum_{j=1}^{k-i-1} \binom{n-2-2i}{j}\binom{n-2-(2i+j)}{k-j-i}\right)$.

(b) *If* $k = |M| - r$, *where* $r = 1,2,3,\dots,\left\lfloor \frac{|M|-3}{2} \right\rfloor$, *then* $\sum_{i=1}^{r} \binom{n-2-i}{n-2-2i}\left(\sum_{j=1}^{k-i-1} \binom{n-2-2i}{j}\binom{n-2-(2i+j)}{k-j-i}\right)$.

(c) *If* $k = |M|$ *then* $(Q_1, Q_2) = 0$.

***Case* (ii) *If* $e_{u_1} \in M_1, e_{u_{n-1}} \notin M_1$, $e_{u_1} \notin M_1$, $e_{u_{n-1}} \in M_1$.**

(a) *If* $3 \le k \le \left\lfloor \frac{|M|+3}{2} \right\rfloor$, *then* $2\left(\begin{array}{c}\sum_{i=1}^{k-2} \binom{n-3-(i-1)}{n-3-2(i-1)} \\ \left(\sum_{j=1}^{k-i-1} \binom{n-3-2(i-1)}{j}\binom{n-3-(2(i-1)+j)}{k-j-i}\right)\end{array}\right)$

(b) *If* $k = |M| - r$, *where* $r = 0,1,2,3,\dots,\left\lfloor \frac{|M|-4}{2} \right\rfloor$ *then* $2\left(\begin{array}{c}\sum_{i=1}^{r+1} \binom{n-3-(i-1)}{n-3-2(i-1)} \\ \left(\sum_{j=1}^{k-i-1} \binom{n-3-2(i-1)}{j}\binom{n-3-(2(i-1)+j)}{k-j-i}\right)\end{array}\right)$.

***Case* (iii) *If* $e_{u_1}, e_{u_{n-1}} \in M_1$.**

(a) *If* $3 \le k \le \left\lfloor \frac{|M|+4}{2} \right\rfloor$, *then* $\sum_{i=2}^{k-2} \binom{n-4-(i-2)}{n-4-2(i-2)}\left(\sum_{j=2}^{k-i-1} \binom{n-4-2(i-2)}{j}\binom{n-4-(2(i-2)+j)}{k-j-i}\right)$.

Published Online First: June, 2024
https://doi.org/10.21123/bsj.2024.10258
P-ISSN: 2078-8665 - E-ISSN: 2411-7986
Baghdad Science Journal

(b) If $k \leq |M| - r$, $where$ $r = 0,1,2,3,\dots,\left\lfloor\frac{|M|-5}{2}\right\rfloor$, $then$ $\sum_{i=2}^{r+2}\binom{n-4-(i-2)}{n-4-2(i-2)}\left(\sum_{j=2}^{k-i-1}\binom{n-4-2(i-2)}{j}\binom{n-4-(2(i-2)+j)}{k-j-i}\right)$.

In the Table 2 below, every possible combination of partitions, partition pairings and k-matchings are listed. It can be observed that when edges in the partitions are paired, more than one set of pairings can result in the same number of k-matchings, since it creates a similar structure in the graph. For this reason, both partitions are labelled in the Table 2.

Table 2. k-matchings of Caterpillar graph CP_n

Partitions	Cases	k-matchings
Q_1	–	$\binom{n-k}{n-2k}$
Q_2 or Q_3	–	$\binom{n-2}{k}$
(Q_2, Q_3)	–	$\sum_{i=1}^{k-1}\binom{n-2}{i}\binom{n-2-1}{k-i}$
(Q_1, Q_2) or (Q_1, Q_3)	(i) $e_{u_1}, e_{u_{n-1}} \notin M_1$	$\sum_{i=1}^{k-1}\binom{n-2-i}{n-2-2i}\binom{n-2-2i}{k-i}$
	(i) $e_{u_1} \in M_1, e_{u_{n-1}} \notin M_1$ (or) (ii) $e_{u_1} \notin M_1, e_{u_{n-1}} \in M_1$	$2\sum_{i=1}^{k-1}\binom{n-3-(i-1)}{n-3-2(i-1)}\binom{n-3-2(i-1)}{k-i}$
	(i) $e_{u_1}, e_{u_{n-1}} \in M_1$	$\sum_{i=2}^{k-1}\binom{n-4-(i-2)}{n-4-2(i-2)}\binom{n-4-2(i-2)}{k-i}$
(Q_1, Q_2, Q_3)	(i) $e_{u_1}, e_{u_{n-1}} \notin M_1$	$2\sum_{i=1}^{k-1}\binom{n-2-i}{n-2-2i}\left(\sum_{j=1}^{k-i-1}\binom{n-2-2i}{j}\binom{n-2-(2i+j)}{k-j-i}\right)$
	(i) $e_{u_1} \in M_1, e_{u_{n-1}} \notin M_1$ (or) (ii) $e_{u_1} \notin M_1$ $e_{u_{n-1}} \in M_1$	$2\left(\sum_{i=1}^{k-2}\binom{n-3-(i-1)}{n-3-2(i-1)}\left(\sum_{j=1}^{k-i-1}\binom{n-3-2(i-1)}{j}\times\binom{n-3-(2(i-1)+j)}{k-j-i}\right)\right)$
	(i) $e_{u_1}, e_{u_{n-1}} \in M_1$	$\sum_{i=2}^{k-2}\binom{n-4-(i-2)}{n-4-2(i-2)}\left(\sum_{j=2}^{k-i-1}\binom{n-4-2(i-2)}{j}\times\binom{n-4-(2(i-2)+j)}{k-j-i}\right)$

Results and Discussion

An example for finding a caterpillar graph CP_6 (Fig 4)[11] has been illustrated below.

Determination of Spectra of CP_6 using results obtained in algebraic Properties of CP_n

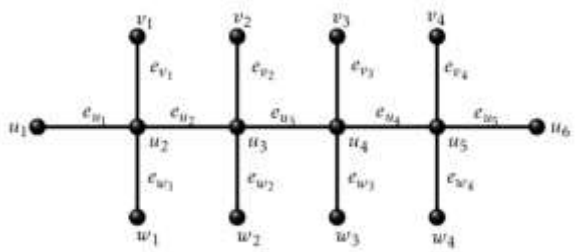

Figure 4. Caterpillar graph (CP_6)[11]

By Theorem 5, the maximum matching $|M| = 4$.

Let us find all k-matching for CP_6 where $k \leq 4$. Here $n = 6$.

1) If $k = 1$. The total number of edges $E(G) = (3n - 5) = 13$.

2) If $k = 2$. By using Theorem 4, 2- matchings $= \frac{9n^2-45n+54}{2} = 54$.

3) If $k = 3$. All the 3-matchings of Caterpillar graph CP_6 is given in Table 3.

Published Online First: June, 2024
https://doi.org/10.21123/bsj.2024.10258
P-ISSN: 2078-8665 - E-ISSN: 2411-7986
Baghdad Science Journal

Table 3. 3-matchings of Caterpillar graph CP_6

Partitions	3-matchings	Number of 3-matchings
Q_1	$\binom{6-3}{6-6}$	1
Q_2	$\binom{6-2}{3}$	4
Q_3	$\binom{6-2}{3}$	4
(Q_1, Q_2)	*Case (i)* $\sum_{i=1}^{1}\binom{4-i}{i}\binom{4-i}{3-i}$	3
	Case (ii) $2\sum_{i=1}^{2}\binom{3-(i-1)}{3-2(i-1)}\binom{3-2(i-1)}{3-i}$	10
	Case (iii) $\sum_{i=2}^{2}\binom{2-(i-2)}{2-2(i-2)}\binom{2-2(i-2)}{3-i}$	2
(Q_1, Q_3)	*Case (i)* $\sum_{i=1}^{1}\binom{4-i}{i}\binom{4-i}{3-i}$	3
	Case (ii) $2\sum_{i=1}^{2}\binom{3-(i-1)}{3-2(i-1)}\binom{3-2(i-1)}{3-i}$	10
	Case (iii) $\sum_{i=2}^{2}\binom{2-(i-2)}{2-2(i-2)}\binom{2-2(i-2)}{3-i}$	2
(Q_2, Q_3)	$\sum_{i=1}^{2}\binom{4}{i}\binom{4-i}{3-i}$	24
(Q_1, Q_2, Q_3)	*Case (i)* $\sum_{i=1}^{1}\binom{4-i}{4-2i}\left(\sum_{j=1}^{1}\binom{4-j}{4-2j}\binom{4-2(i+j)}{3-j-i}\right)$	6
	Case(ii) $2\left(\sum_{i=1}^{1}\binom{3-(i-1)}{3-2(i-1)}\left(\sum_{j=1}^{1}\binom{3-2(i-1))}{j}\times\binom{3-(2(i-1)+j)}{3-i-j}\right)\right)$	12
	Case (iii) $\left(\sum_{i=1}^{2}\binom{2-(i-1)}{2-2(i-1)}\left(\sum_{j=1}^{2}\binom{2}{j}\binom{2-(2(i-2)+j)}{4-i-j}\right)\right)$	0
	Total number of 3- matchings	81

4) If $k = 4$. All the 4-matchings of Caterpillar graph CP_6 is given in Table 4.

Table 4. 4-matchings of Caterpillar graph CP_6

Partitions	4-matchings	Number of 3-matchings
Q_1	$\binom{6}{2}<4$	0
Q_2	$\binom{6-2}{4}$	1
Q_3	$\binom{6-2}{4}$	1
(Q_1, Q_2)	*Case (i)* $2<4$	0
	Case (ii) $2\sum_{i=1}^{1}\binom{3-(i-1)}{3-2(i-1)}\binom{3-2(i-1)}{4-i}$	2
	Case (iii) $\sum_{i=2}^{2}\binom{2-(i-2)}{2-2(i-2)}\binom{2-2(i-2)}{4-i}$	1
(Q_1, Q_3)	*Case (i)* $2<4$	0
	Case (ii) $\sum_{i=1}^{1}\binom{3-(i-1)}{3-2(i-1)}\binom{3-2(i-1)}{4-i}$	2

Published Online First: June, 2024
https://doi.org/10.21123/bsj.2024.10258
P-ISSN: 2078-8665 - E-ISSN: 2411-7986
Baghdad Science Journal

	Case (iii) $\sum_{i=2}^{2}\binom{2-(i-2)}{2-2(i-2)}\binom{2-2(i-2)}{4-i}$	1
(Q_2, Q_3)	$\sum_{i=1}^{2}\binom{4}{i}\binom{4-i}{3-i}$	14
(Q_1, Q_2, Q_3)	*Case (i)* $\sum_{i=1}^{1}\binom{4-i}{4-2i}\left(\sum_{j=1}^{1}\binom{4-j}{4-2j}\binom{4-2(i+j)}{3-j-i}\right)$	0
	Case(ii) $2\left(\sum_{i=1}^{1}\binom{3-(i-1)}{3-2(i-1)}\left(\sum_{j=1}^{1}\binom{3-2(i-1))}{j}\times\binom{3-(2(i-1)+j)}{3-i-j}\right)\right)$	12
	Case (iii) $\left(\sum_{i=1}^{2}\binom{2-(i-1)}{2-2(i-1)}\left(\sum_{j=1}^{2}\binom{2}{j}\binom{2-(2(i-2)+j)}{4-i-j}\right)\right)$	2
	Total number of 4- matchings	36

Thus, all k-matchings of Caterpillar graph CP_6 is calculated. From the above list of computations and by using Lemma 1, the following spectral parameters of CP_6 are found.

$$P(A;\lambda) = \lambda^{14} - 13\lambda^{12} + 54\lambda^{10} - 81\lambda^{8} + 36\lambda^{6}.$$

$$P(A;\lambda) = \lambda^{6}(\lambda-2)\ (\lambda+2)(\lambda^{3} - 3\lambda^{2} + 3)(\lambda^{3} + 3\lambda^{2} - 3).$$

$$Sp(CP_6) = \{\pm 2.531^{(1)}, \pm 2^{(1)}, \pm 1.3473^{(1)}, \pm 0.8794^{(1)}, 0^{(6)}\}.$$

Similarly, the following characteristic polynomials of Caterpillar graph CP_n, $3 \le n \le 10$ are derived.

If $n = 3$ $P(A;\ \lambda) = \lambda^{5} - 4\lambda^{3}$.

If $n = 4$ $P(A;\ \lambda) = \lambda^{8} - 7\lambda^{6} + 9\lambda^{4}$.

If $n = 5$ $P(A;\ \lambda) = \lambda^{11} - 10\lambda^{9} + 27\lambda^{7} - 18\lambda^{5}$.

If $n = 6$ $P(A;\ \lambda) = \lambda^{14} - 13\lambda^{12} + 54\lambda^{10} - 81\lambda^{8} + 36\lambda^{6}$.

If $n = 7$ $P(A;\ \lambda) = \lambda^{17} - 16\lambda^{15} + 90\lambda^{13} - 216\lambda^{11} + 216\lambda^{9} - 72\lambda^{7}$.

If $n = 8$ $P(A;\ \lambda) = \lambda^{20} - 19\lambda^{18} + 135\lambda^{16} - 450\lambda^{14} + 729\lambda^{12} - 540\lambda^{10} + 144\lambda^{8}$.

If $n = 9$ $P(A;\ \lambda) = \lambda^{23} - 22\lambda^{21} + 189\lambda^{18} - 810\lambda^{17} + 1845\lambda^{15} - 2214\lambda^{13} + 1296\lambda^{11} - 288\lambda^{9}$.

If $n = 10$ $P(A;\ \lambda) = \lambda^{26} - 25\lambda^{24} + 252\lambda^{22} - 1323\lambda^{20} + 3915\lambda^{18} - 6633\lambda^{16} + 6264\lambda^{14} - 3024\lambda^{12} + 576\lambda^{10}$.

By solving the above polynomials and arranging the eigenvalues along with its algebraic multiplicities the following spectrum of CP_n, , $3 \le n \le 10$ has been obtained.

$$Sp(CP_3) = \{\pm 2^{(1)}, 0^{(3)}\}.$$

$$Sp(CP_4) = \{\pm 2.3028^{(1)}, \pm 1.3028^{(1)}, 0^{(4)}\}.$$

$$Sp(CP_5) = \{\pm 2.4495^{(1)}, \pm 1.7321^{(1)}, \pm 1^{(1)}, 0^{(5)}\}.$$

$$Sp(CP_6) = \{\pm 2.531^{(1)}, \pm 2^{(1)}, \pm 1.3473^{(1)}, \pm 0.8794^{(1)}, 0^{(6)}\}.$$

$$Sp(CP_7) = \{\pm 2.5832^{(1)}, \pm 2.1753^{(1)}, \pm 1.6273^{(1)}, \pm 1.1260^{(1)}, \pm 0.8241^{(1)}, 0^{(7)}\}.$$

$$Sp(CP_8) = \{\pm 2.6170^{(1)}, \pm 2.2954^{(1)}, \pm 1.8396^{(1)}, \pm 1.3663^{(1)}, \pm 1^{(1)}, \pm 0.7948^{(1)}, 0^{(8)}\}.$$

$$Sp(CP_9) = \{\pm 2.6404^{(1)}, \pm 2.3810^{(1)}, \pm 2^{(1)}, \pm 1.5735^{(1)}, \pm 1.1931^{(1)}, \pm 0.9246^{(1)}, \pm 0.7775^{(1)}, 0^{(9)}\}.$$

$$Sp(CP_{10}) = \{\pm 2.6574^{(1)}, \pm 2.4439^{(1)}, \pm 2.1227^{(1)}, \pm 1.7451^{(1)}, \pm 1.3769^{(1)}, \pm 1.0782^{(1)}, \pm 0.8767^{(1)} \pm 0.7665^{(1)}, 0^{(10)}\}$$

The spectral parameters calculated from the above result are listed in the following Table 5.

Published Online First: June, 2024
https://doi.org/10.21123/bsj.2024.10258
P-ISSN: 2078-8665 - E-ISSN: 2411-7986
Baghdad Science Journal

Table 5. Spectral parameters of CP_n

CP_n	Spectral radius	Second largest eigenvalues	Spectral gap	Graph energy	Eigenvalue-based entropy
CP_3	2	0	2	4	0.3010
CP_4	2.3028	1.3028	1	7.2111	0.5851
CP_5	2.4495	1.7321	0.7174	10.3631	0.7518
CP_6	2.531	2	0.531	13.5175	0.8721
CP_7	2.5832	2.1753	0.4079	16.6718	0.9662
CP_8	2.6170	2.2954	0.3216	19.8216	1.0436
CP_9	2.6404	2.3810	0.2594	22.9804	1.1092
CP_{10}	2.6574	2.4439	0.2135	26.1347	1.1662
CP_{11}	2.6701	2.4915	0.1786	29.2890	1.2166
CP_{12}	2.6798	2.5282	0.1516	32.4433	1.2617
CP_{13}	2.6874	2.5572	0.1302	35.5976	1.3026
CP_{14}	2.6934	2.5805	0.1129	38.7519	1.3400
CP_{15}	2.6983	2.5994	0.0989	41.9026	1.3744
CP_{16}	2.7024	2.6151	0.0873	45.0605	1.4063
CP_{17}	2.7057	2.6281	0.0776	48.2148	1.4360
CP_{18}	2.7085	2.6391	0.0694	51.3691	1.4638
CP_{19}	2.7109	2.6484	0.0625	54.5234	1.4899
CP_{20}	2.7129	2.6564	0.0565	57.6777	1.5145
CP_{21}	2.7147	2.6633	0.0514	60.8302	1.5379
CP_{22}	2.7168	2.6693	0.0475	63.9863	1.5600
CP_{23}	2.7176	2.6745	0.0431	67.1406	1.5810
CP_{24}	2.7181	2.6792	0.0389	70.2949	1.6011
CP_{25}	2.7198	2.6833	0.0365	73.4492	1.6203
CP_{26}	2.7207	2.6869	0.0338	76.6035	1.6387
CP_{27}	2.7215	2.6901	0.0314	79.7578	1.6563
CP_{28}	2.7222	2.6930	0.0292	82.9121	1.6733
CP_{29}	2.7229	2.6957	0.0272	86.0663	1.6896
CP_{30}	2.7235	2.6980	0.0255	89.2206	1.7053
CP_{31}	2.7240	2.7002	0.0238	92.3749	1.7205
CP_{32}	2.7245	2.7021	0.0224	95.5292	1.7352
CP_{33}	2.7250	2.7039	0.0211	98.6835	1.7493
CP_{34}	2.7254	2.7055	0.0199	101.8378	1.7631
CP_{35}	2.7258	2.7070	0.0188	104.9921	1.7764

From the above parameters the following graphs (Fig 5) have been obtained using MATLAB to have a comparative view among the results obtained.

Published Online First: June, 2024
https://doi.org/10.21123/bsj.2024.10258
P-ISSN: 2078-8665 - E-ISSN: 2411-7986
Baghdad Science Journal

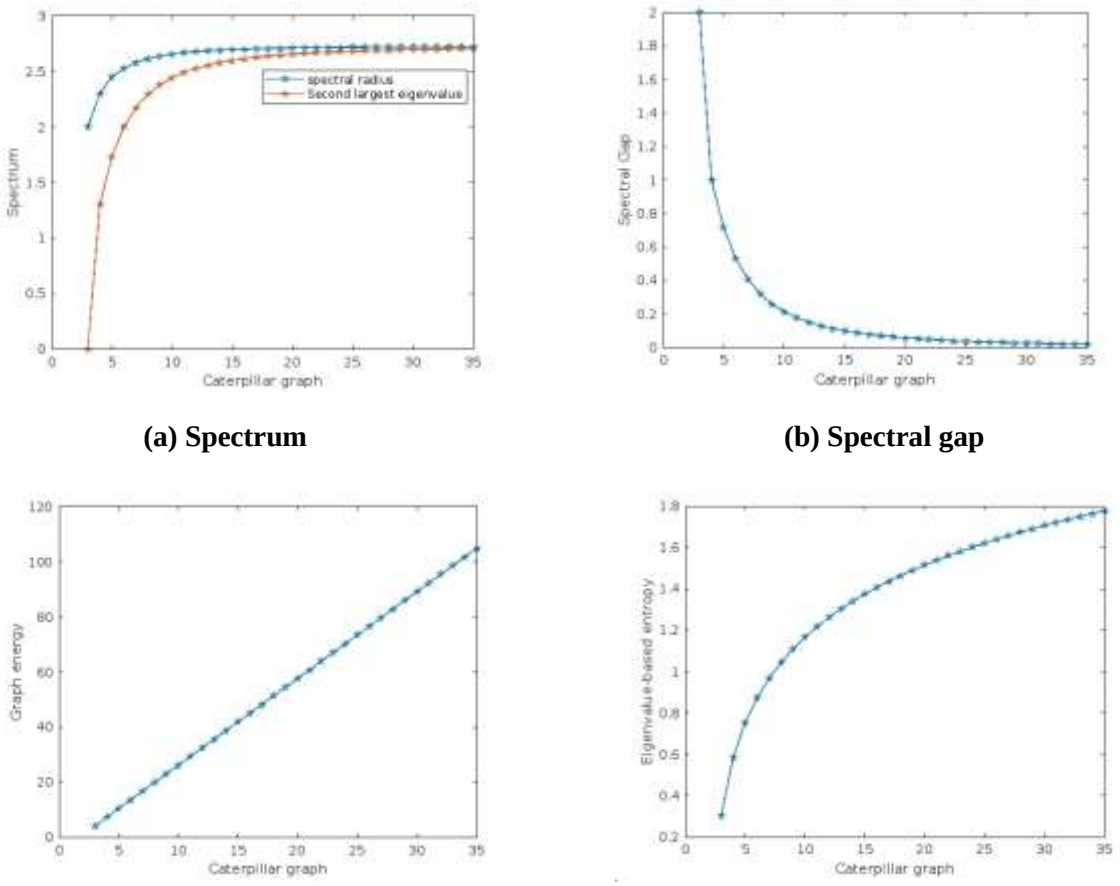

(a) Spectrum **(b) Spectral gap**

(c) Graph energy **(d) Eigenvalue-based entropy**

Figure 5. Graphical representation of spectral parameters in Table 3

Observations

1. For any positive integer $n \geq 3$, CP_n has eigenvalue zero with algebraic multiplicity n, whereas other
2. eigenvalues are simple.
3. Since the maximum degree of the graph is 4 the spectral radius $\rho(CP_n) \leq 4$.
4. When $n \equiv 0 \pmod 3$, 2 is an eigenvalue of CP_n with multiplicity 1.
5. When $n \equiv 2 \pmod 3$, 1 occurs as an eigenvalue of CP_n.
6. The spectral radius and the second largest eigenvalue converges between 2.5 to 3 and spectral gap converges to zero.
7. The maximum spectral gap of caterpillar graph is atmost 2.

Conclusion

This study determines the spectral parameters and graph entropies of special caterpillar graphs that occur in Chemistry and their graph families. The results were represented graphically for quick and easy analysis. This research enhances our understanding of the spectral characteristics and graph entropies for the aforementioned graph families.

Published Online First: June, 2024
https://doi.org/10.21123/bsj.2024.10258
P-ISSN: 2078-8665 - E-ISSN: 2411-7986
Baghdad Science Journal

Acknowledgment

The corresponding author, A. A, would like to thank SRM Institute of Science and Technology, Kattankulathur, Tamil Nadu, India for supporting her research under "Selective Excellence Research Initiative-2021" grant.

Authors' Declaration

- Conflicts of Interest: None.
- We hereby confirm that all the Figures and Tables in the manuscript are ours. Furthermore, any Figures and images, that are not ours, have been included with the necessary permission for re-publication, which is attached to the manuscript.
- No animal studies are present in the manuscript.
- No human studies are present in the manuscript.
- Ethical Clearance: The project was approved by the local ethical committee at SRM Institute of Science and Technology, Kattankulathur 603203, Tamil Nadu, India.

Authors' Contribution Statement

B. I. A and A. A contributed equally to the design and implementation of the research, to the analysis of the results and to the writing of the manuscript.

References

1. Wagner, Stephan, Hua Wang. Introduction to Chemical Graph Theory. Florida: CRC Press Taylor & Francis Group; 2018 Sep 5. p. 1-10. https://doi.org/10.1201/9780429450532.
2. Sun Y, Zhao H. Eigenvalue-based entropy and spectrum of bipartite digraph. Complex Intell Syst. 2022 Sep 20; 8(4): 3451–3462. https://doi.org/10.1007/s40747-022-00679-9.
3. Balakrishnan R, Ranganathan K A Textbook of Graph Theory. 2nd Ed. New York Heidelberg Dordrecht London: Springer Science & Business Media; 2012. p. 261-267. https://doi.org/10.1007/978-1-4614-4529-6.
4. Dehmer M. Information processing in complex networks: Graph entropy and information functionals. Appl Math Comput. 2008 Jul 15; 201(1-2): 82–94. https://doi.org/10.1016/j.amc.2007.12.010.
5. Brouwer AE, Haemers WH. Spectra of Graphs. New York Heidelberg Dordrecht London: Springer Science & Business Media Springer; 2011 Dec 17. p. 1-17. https://doi.org/10.1007/978-1-4614-1939-6_1.
6. Celik F, Cangül İ. On the spectra of cycles and paths. TWMS J Appl Eng Math. 2019 Jul 1; 9(3): 571–580.
7. Alwan NA, Al-Saidi NM. A general formula for characteristic polynomials of some special graphs. Eng. & Tech J. 2016 May 1; 34(5): 638–650.
8. Gutman I, Trinajstić N. Graph theory and molecular orbitals. Total φ-electron energy of alternant hydrocarbons. Chem Phys Lett. 1972 Dec 15; 17(4): 535–538. https://doi.org/10.1016/0009-2614(72)85099-1.
9. Anwar S, Jamil MK, Alali AS, Zegham M, Javed A. Extremal values of the first reformulated Zagreb index for molecular trees with application to octane isomers. AIMS Math 2024; 9(1): 289-301. http://dx.doi.org/10.3934/math.2024017.
10. Mitesh JP, Kajal SB, Ashika .P. More on second Zagreb energy of graphs. Open J Discret Appl Math. 2023 Dec 27. 2(4): 7 – 13. http://dx.doi.org/10.30538/psrp-odam2023.0084.
11. Dobrynin AA, Estaji E. Wiener index of hexagonal chains under some transformations. Open J Discret Appl Math. 2020 Dec 31; 3(1): 28-36. https://doi:10.30538/psrp-odam2020.0027.
12. Noor M, Jamil MK, Ullah K, Azeem M, Pamucar D, Almohsen B. Energies of T-spherical fuzzy graph based on novel Aczel-Alsina T-norm and T-conorm with their applications in decision making. J Intell Fuzzy Syst. 2023 Jan 1. 45(6): 9363 – 9385. http://dx.doi.org/ 10.3233/JIFS-231086.
13. Waheed M, Saleem U, Javed A, Jamil MK. Computational aspects of entropy measures for metal organic frameworks. Mol Phys. 2023 Sep 7: e2254418. https://doi.org/10.3390/molecules28124726 .
14. Al-Janabi H, Bacs´o G. Sanskruti Index of some Chemical Trees and Unicyclic Graphs. J Phys Conf Ser. 2022 Jun 1; 2287: 012005. https://doi.org/10.1088/1742-6596/2287/1/012005 .
15. Lin Z. Connectivity indices and QSPR analysis of benzenoid hydrocarbons. Open J Discret Appl Math. 2023 Dec 27. 3(2): 35 – 40. https://doi.org/10.30538/psrp-odam2023.0092 .
16. Ahmad Z, Naseem M, Jamil MK, Siddiquid MK, Nadeemd MF. New results on eccentric connectivity indices of V-Phenylenic nanotube. Eurasian Chem Commun. 2020 June 1; 6(3): 663-71. http://dx.doi.org/10.33945/SAMI/ECC.2020.6.3

Published Online First: June, 2024
https://doi.org/10.21123/bsj.2024.10258
P-ISSN: 2078-8665 - E-ISSN: 2411-7986
Baghdad Science Journal

17. Raja NJMM, Anuradha A. Topological entropies of single walled carbon nanotubes. J. Math. Chem. 2023 Nov 2: 1-0. https://doi.org/10.1007/s10910-023-01532-1
18. Raja NJMM, Anuradha A. On Sombor indices of generalized tensor product of graph families. Results Control Optim. 2024 Jan 10: 100375. https://doi.org/10.1016/j.rico.2024.100375 .
19. Devaragudi V, Chaluvaraju B. Block Sombor index of a graph and its matrix representation. Open J Discret Appl Math. 2023 Apri 30; 6(1): 1-11. http://dx.doi.org/10.30538/psrp-odam2023.0078.
20. Jamil MK, Imran M, Abdul Sattar K. Novel face index for benzenoid hydrocarbons. Mathematics. 2020 Mar 1; 8(3): 312. http://dx.doi.org/doi:10.3390/math8030312.
21. Zhang X, Waheed M, Jamil MK, Saleemd U, Javed A. Entropy measures of the metal–organic network via topological descriptors. Main Group Met Chem. 2023 Dec 12; 46(1): 20230011. https://doi.org/10.1515/mgmc-2023-0011 .
22. Sardar MS, Siddique I, Jarad F, Ali MA, Türkan EM, Danish, M. Computation of vertex-based topological indices of middle graph of alkane. J Math. 2022; 2022(3): 24. https://doi.org/10.1155/2022/8283898 .
23. Sardar M S, Ali M A, Farahani M R, Alaeiyan M, Cancan M. Degree-based topological indices of alkanes by applying some graph operations. Eur Chem Bull. 2023; 12(5): 39-50. https://doi.org/10.31838/ecb/2023.12.si5.004 .
24. Puruchothama MN, Simon F. Diagrammatic representation between topological indices and alkanes. J Algebr Stat. 2022 Jul 23; 13(2): 3536–3545.
25. Lakshmi KV, Parvathi N. An analysis of thorn graph on topological indices. IAENG Int J Appl Math. 2023 Sep 1; 53(3): 1084-1093.
26. Javaid M, Siddique MK, Bonyah E. Computing Gutman connection index of thorn graphs. J Math. 2021 Nov 15; 2021(6): 11. https://doi.org/10.1155/2021/2289514 .
27. Chithra KP, Mayamma J. Total global dominator coloring of trees and unicyclic graphs. Baghdad Sci J. 2023; 20(4): 1380-1386. https://doi.org/10.21123/bsj.2023.6457 .
28. Ali AM, Ahmed HJ, Saleh GAM. Detour polynomials of generalized vertex identified of graphs. Baghdad Sci J. 2023 Apr 1; 20(2): 0343–0343. https://doi.org/10.21123/bsj.2022.6350 .
29. Ouellette RJ, Rawn JD. Organic Chemistry: Structure, Mechanism, Synthesis. Academic Press; 2018 Feb 3. p 87-133. https://doi.org/10.1016/C2016-0-04004-4 .
30. Clark GJ, Cooper JN. A Harary-Sachs theorem for hypergraphs. J Comb Theory Ser B. 2021 Jul 1; 149(1): 1–15. https://doi.org/10.1016/j.jctb.2021.01.002 .

اليرقات الخاصة في الكيمياء ورؤاها البيانية الطيفية

بي آي أندرو، أ. أنورادها

قسم الرياضيات، كلية الهندسة والتكنولوجيا، معهد SRM للعلوم والتكنولوجيا، كاتانكولاثر 603203، تاميل نادو، الهند.

الخلاصة

لا غنى عن نظرية الرسم البياني الكيميائي لنمذجة الجزيئات، لا سيما في الألكانات، وهي فئة من الهيدروكربونات ذات الصيغة C_nH_{2n+2}. تظهر أيزومرات الألكانات تنوعًا هيكليًا على الرغم من مشاركتها في نفس الصيغة الكيميائية، مما يؤدي إلى خصائص طيفية مميزة. تعتبر واصفات الرسوم البيانية محورية في كيمياء الكم، حيث توفر الأدوات الأساسية للتحليل. تلعب المعلمات الطيفية، بما في ذلك نصف القطر الطيفي، وثاني أكبر القيم الذاتية، والفجوة الطيفية، وطاقة الرسم البياني، دورًا حاسمًا في تقدير مستويات الطاقة والاستقرار الجزيئي. إنتروبيا الرسم البياني، مثل إنتروبيا المعامل القائم على القيمة الذاتية المستمدة من مصفوفة المجاورة، تحدد كمية عدم التجانس الجزيئي. تركز هذه الورقة على نوع معين من الألكانات وايزومراتها، وتحليل معاملاتها الطيفية والانتروبيا البيانية. وتستخدم الرسوم البيانية المقارنة لتوضيح طبيعة هذه المعلمات، وكشف تعقيدات السلوك الجزيئي. تؤكد الدراسة على أهمية نظرية الرسم البياني في كيمياء الكم، وخاصة في فهم الخصائص الطيفية والتعقيدات الهيكلية للألكانات وإيزومراتها. ويساهم هذا الفهم بشكل كبير في الفهم الشامل للخصائص الجزيئية والسلوك على المستوى الكمي، مما يؤكد الدور الحيوي لنظرية الرسم البياني الكيميائي في البحث العلمي الحديث.

الكلمات المفتاحية: أيزومرات الألكان، الرسم البياني كاتربيلر، الإنتروبيا القائمة على القيمة الذاتية، الرسم البياني للطاقة، والطيف البياني.